D2SA: Dual-Stage Distribution and Slice Adaptation for Efficient Test-Time Adaptation in MRI Reconstruction

Lipei Zhang[1*], Rui Sun[2*], Zhongying Deng[1], Yanqi Cheng[1],

Carola-Bibiane Schonlieb[1], Angelica I Aviles-Rivero[3]

1. Department of Applied Mathematics and Theoretical Physics, University of Cambridge
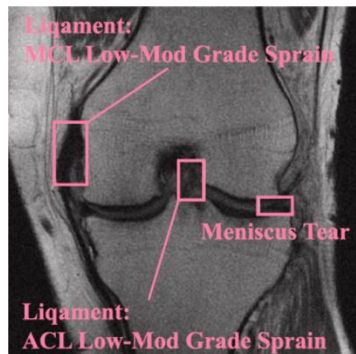2. School of Science and Engineering (SSE), The Chinese University of HongKong, ShenZhen
3. Yau Mathematical Sciences Center, Tsinghua University
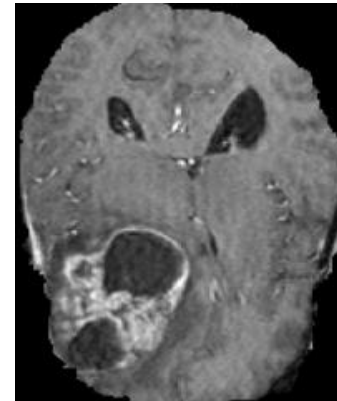
Outline

- Background

  - Magnetic Resonance Imaging (MRI)

  - Problem setup in MRI Reconstruction

  - Domain shift in MRI Reconstruction

- Related works

- Proposed Method and Mathematical Analysis

- Experimental Results

- Conclusion

UNIVERSITY OF CAMBRIDGE

Background

- ## Magnetic Resonance Imaging (MRI)

  - Invasive, harmless

  - Accurate, high-resolution, reproducible

 - Providing various contrasts and functional information

Knee MRI [1,2]

Brain MRI [3]
(Glioma)

[1] Huang, J et al,. Enhancing global sensitivity and uncertainty quantification in medical image reconstruction with Monte Carlo arbitrary-masked mamba. MedIA, 2025
[2] FastMRI-Plus, https://github.com/microsoft/fastmri-plus
[3] F. Isensee et al,. 'Brain Tumor Segmentation and Radiomics Survival Prediction: Contribution to the BRATS 2017 Challenge'. arXiv, 2018.

UNIVERSITY OF CAMBRIDGE

Background

- Magnetic Resonance Imaging (MRI)

- Raw data Collection: in Fourier space (k-space)

- Fully Sample: Time-consuming, artefact

- Undersample + Reconstruction:

  - Parallel Imaging: SENSE, GRAPPA……

  - **Compressed Sensing: TV, ADMM……**

  - **Deep Learning ……**
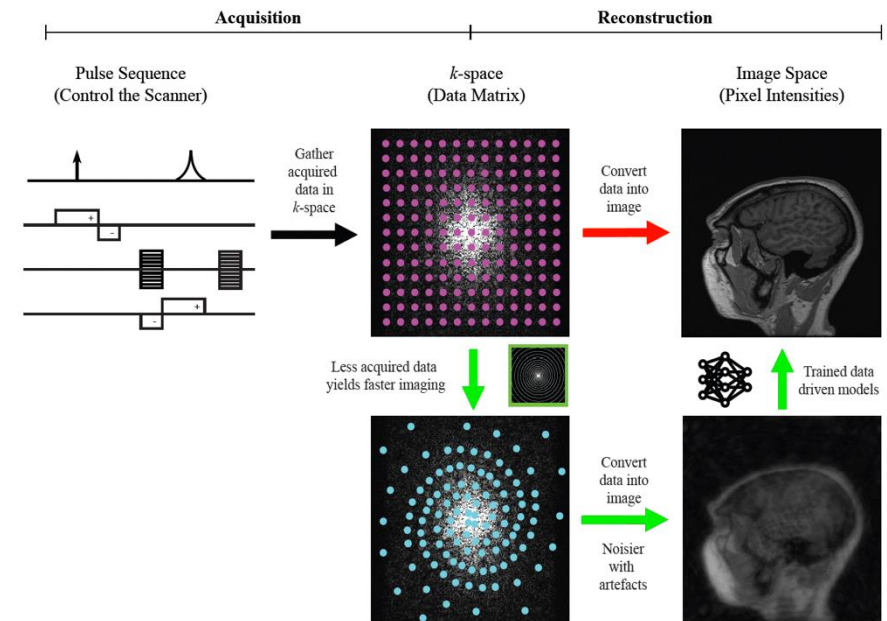
Sampling masks:
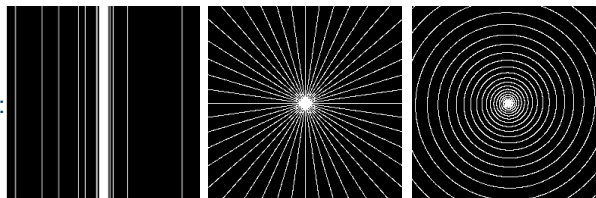
Cartesian   Radial   Spiral
(Commonly used)

Background

- ## Problem in MRI Reconstruction

- **MRI reconstruction** is formulated as an **inverse problem**:
  Recover $x^* \in \mathbb{C}^n$ from $y \in \mathbb{C}^m$, $M \ll N$, A is is the measurement operator, and ϵ represents noise.

$$y = A\,x^* + \epsilon$$

- **For Multi-coil MRI,** we can expend A containing S coil sensitivity maps, F is the 2D Fourier transform, and M is the undersampling mask.

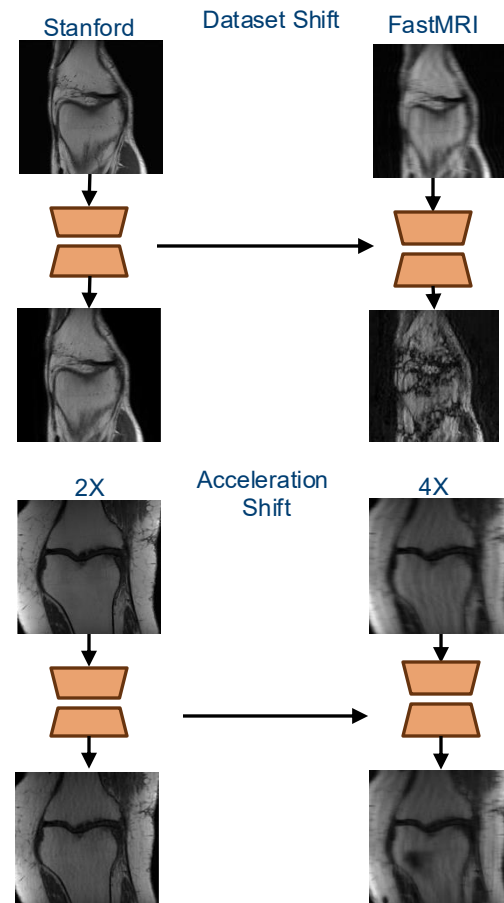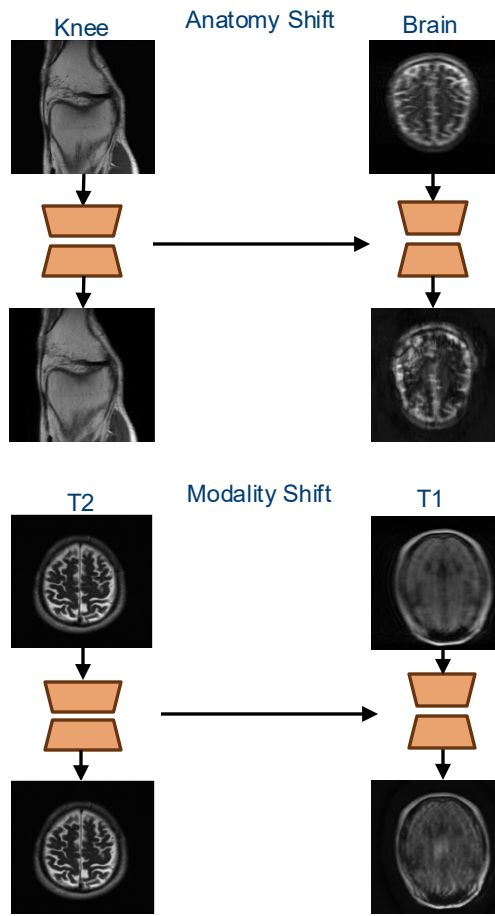$$y_i = M\,F'\,S_i\,x^* + \epsilon, \quad i = 1, \ldots, n_c$$

- **Optimisation for reconstruction**

$$\hat{x} = \arg\min_x \ \tfrac{1}{2}\|A\,x - y\|_2^2 + \lambda R(x)$$

where R(x) encodes prior knowledge (e.g., wavelet ℓ1, total variation, or CNN-based priors), and λ controls the balance between data fidelity and regularisation.

Background

- Domain shifts in MRI Reconstruction

Background

- Three key goals for overcoming domain shifts

  1. Strong adaptation to new distributions

     ✓ Maintaining high performance despite distribution shifts.

  2. Robustness to limited data

     ✓ Preventing overfitting in medical data-scarce scenarios

  3. Fast convergence

     ✓ Minimizing adaptation time

- Solution: Test-time Adaptation

  ✓ No label in test-time

  ✓ No access to source dataset (distribution information or images)

  ✓ Adapt multiple domain shifts

Background

- ## Test-time Adaptation

  - ### Previous works

    - **Single** iterative sampling

      - Score-based prior and Langevin dynamic [3]
      - Hyperparameters may not generalize well to test settings and strong assumption

    - **Single**-shot iterative method

      - Deep image prior based method (c; [4])
      - Repeated test-time trainings

    - **Batch** unrolled adaptation for inverse optimisation (a[1]; b[2])

      - Only suitable for parametric changes (mask and acc ratio)

    - **Batch** self-supervised method

      - FINE[5], Noiser2Noise [6], SSDU (d; [7])
      - Over-smoothing; require enough data

a.

(a) Original reconstruction network.

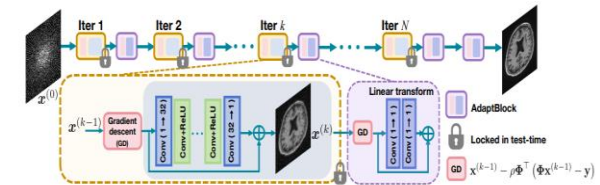$$y \rightarrow f_0 \rightarrow \hat{x} = f_0(y) = f(y; \theta_0, A_0)$$

(b) Model adaptation by Parametrize and Perturb (P&P).

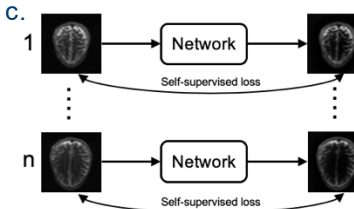$$y \rightarrow f_1 \rightarrow \hat{x} = f_1(y) = f(y; \theta_0 + \delta, A_1)$$

(c) Model adaptation by Reuse & Regularize (R&R).

b.

$$GD \quad x^{(k-1)} - \beta \Phi^\top (\Phi x^{(k-1)} - y)$$

c.

d.

[1] G. Davis et al., "Model Adaptation for Inverse Problems in Imaging", IEEE TRANSACTIONS ON COMPUTATIONAL IMAGING 2021
[2] Zhao Y et al., "Test-Time Model Adaptation for Image Reconstruction Using Self-supervised Adaptive Layers", ECCV 2024
[3] J. Ajil et al., "Robust Compressed Sensing MRI with Deep Generative Priors ", NeurIPS 2021
[4] D. Mohammad et al., "Test-Time Training Can Close the Natural Distribution Shift Performance Gap in Deep Learning Based Compressed Sensing", ICML, 2022
[5] Zhang J et al., "Fidelity imposed network edit (fine) for solving ill-posed image reconstruction", Neuroimage 2020
[6] Moran N et al., "Learning to Denoise From Unpaired Noisy Data", CVPR 2020
[7] Yaman B et al., "Self-supervised learning of physics-guided reconstruction neural networks without fully sampled reference data", Magnetic resonance in medicine 2020

Background

- Test-time Adaptation
  - ➢ Single-slice training

Source

Target

Slow convergence

Repeated training

x_1

x_2

$x_{\dots}$

x_3

Unstable shift

a. single-slice approach
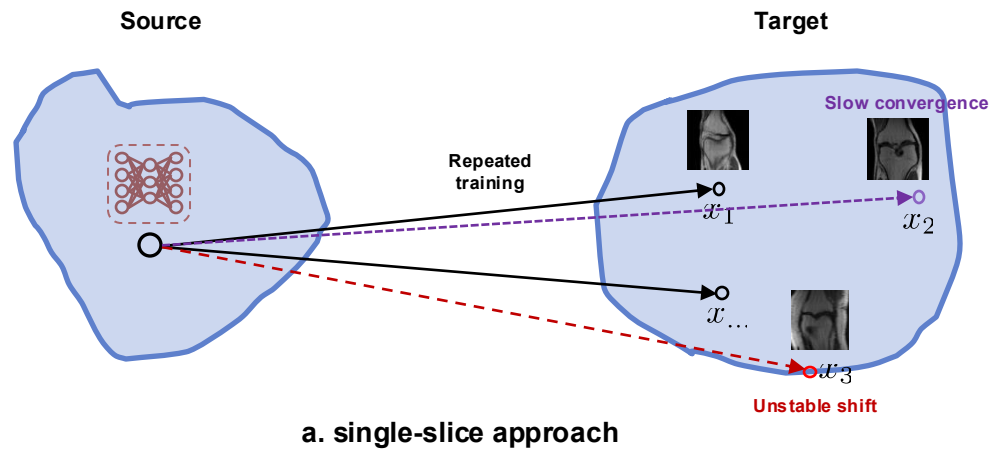
Background

- Test-time Adaptation

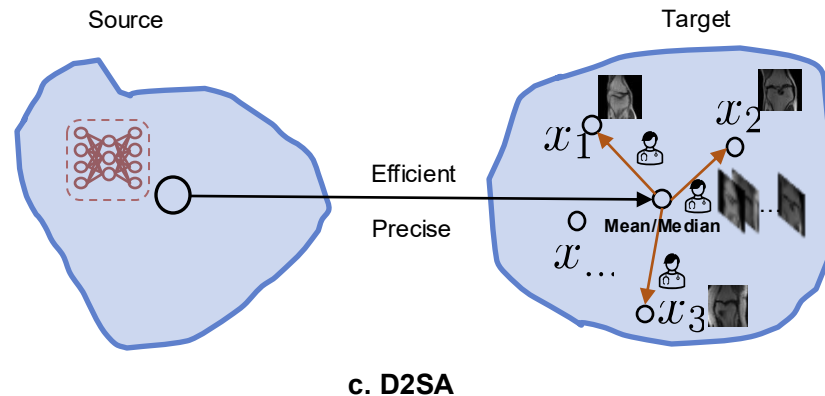 ➤ Batch/mini-batch training
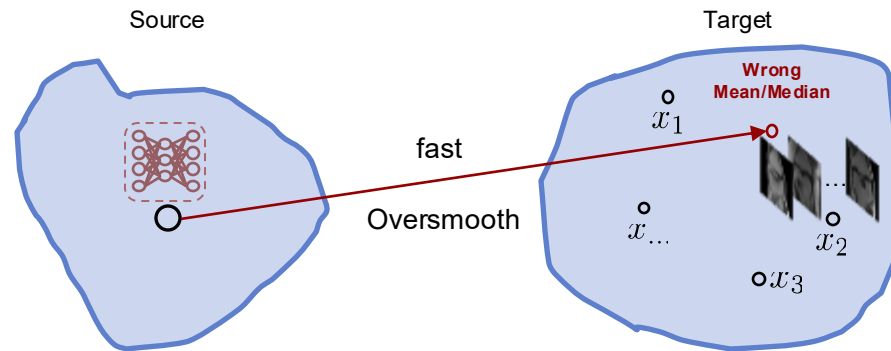
b. Self-supervised approach with few data

Background

- ## Test-time Adaptation

  - Can we use Batch training + single training?

    - ✓ Good pretrained weight [1]

    - ✓ Meta-learning [2]

    - ✓ Faster convergence [3]

  - Our proposed test-time adaptation (D2SA: Dual-Stage Distribution and Slice Adaptation)

   1. Patient-level Adaptation

    2. Single-Slice Refinement

c. D2SA

[1] Barbano, R et al,. 'An Educated Warm Start for Deep Image Prior-Based Micro CT Reconstruction'. IEEE Transactions on Computational Imaging, 2022
[2] Zhang K et al,. 'MetaDIP: Accelerating Deep Image Prior with Meta Learning'. Arxiv, 2022
[3] Onishi Y et al,. 'Self-Supervised Pre-Training for Deep Image Prior-Based Robust PET Image Denoising'. IEEE Transactions on Radiation and Plasma Medical Sciences, 2024.

UNIVERSITY OF CAMBRIDGE

Related Works

- Implicit Neural Network (INR)

  ➢ Model single data as **continuous** implicit functions, providing critical advantages such as **resolution independence, no label, memory efficiency, and generalisation** beyond discretised data structures. [1]
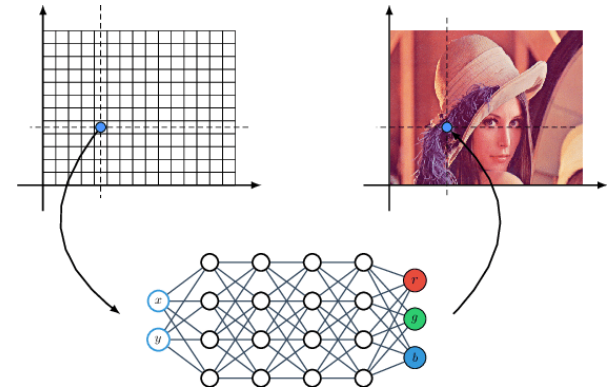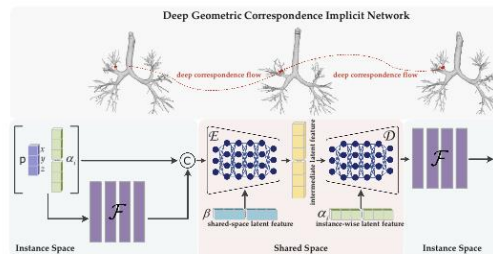
- Function-level Domain Representation Learning

  ➢ From data to functa [2]: latent modulations **(latent vector + coordinate)**
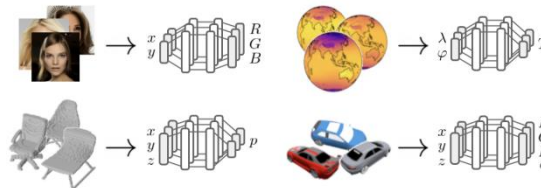
  ➢ DeepSDF learns continuous signed distance functions (SDFs) [3]

  ➢ INR for topological features in medical field [4]

[1] Essakine A et al,. "Where Do We Stand with Implicit Neural Representations? A Technical and Performance Survey". TMLR, 2025
[2] Dupont E et al,. "From data to functa: Your data point is a function and you can treat it like one", ICML 2022
[3] Park J et al,. "Deepsdf: Learning continuous signed distance functions for shape representation", CVPR 2019
[4] Zhang M et al., "Implicit Representation Embraces Challenging Attributes of Pulmonary Airway Tree Structures", MICCAI 2024

UNIVERSITY OF CAMBRIDGE

Related Works

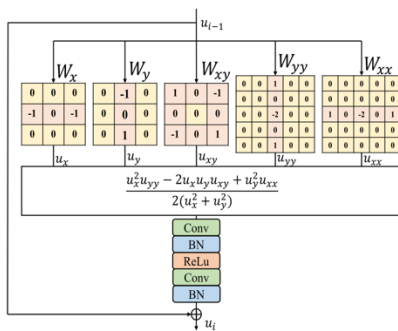- Anisotropic Diffusion (AD) Equation (Perona-Malik equation)

  ➢ A non-linear image smoothing technique that reduces noise while preserving sharp edges and other important features [1]

$$\begin{cases} \left(\frac{\partial u}{\partial t}\right) = \text{div}\left(g(|\nabla u|)\nabla u\right) \\ g(|\nabla u|) = \frac{1}{1 + \frac{|\nabla u|^2}{k^2}} \end{cases} \tag{1}$$
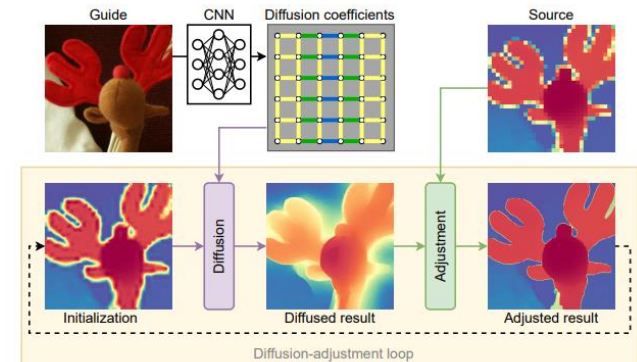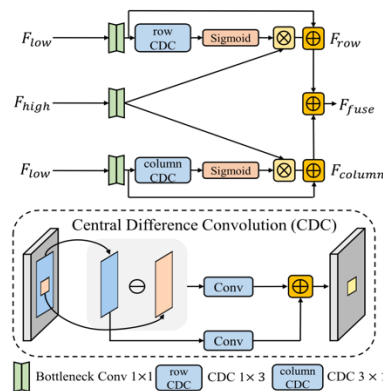
When the gradient magnitude is small ($|\nabla u| \to 0$), the diffusion coefficient g approaches one, leading to isotropic smoothing. Near object boundaries, where $|\nabla u| \to 1$, g approaches zero, preventing diffusion and preserving fine details.

 ➢ Applications in deep learning methods

  1. Small Target Detection [2]

  2. Super-resolution [3]

[1] Pietro Perona and Jitendra Malik. "Scale-space and edge detection using anisotropic diffusion". IEEE Transactions on Pattern Analysis and Machine Intelligence 1990.
[2] Chen T et al,. "eature preservation and shape cues assist infrared small target detection", IEEE Transactions on Geoscience and Remote Sensing, 2024
[3] Metzger N et al, . "Guided Depth Super-Resolution by Deep Anisotropic Diffusion", CVPR 2023

UNIVERSITY OF CAMBRIDGE

Proposed Method

- D2SA: TTA Framework-Overview
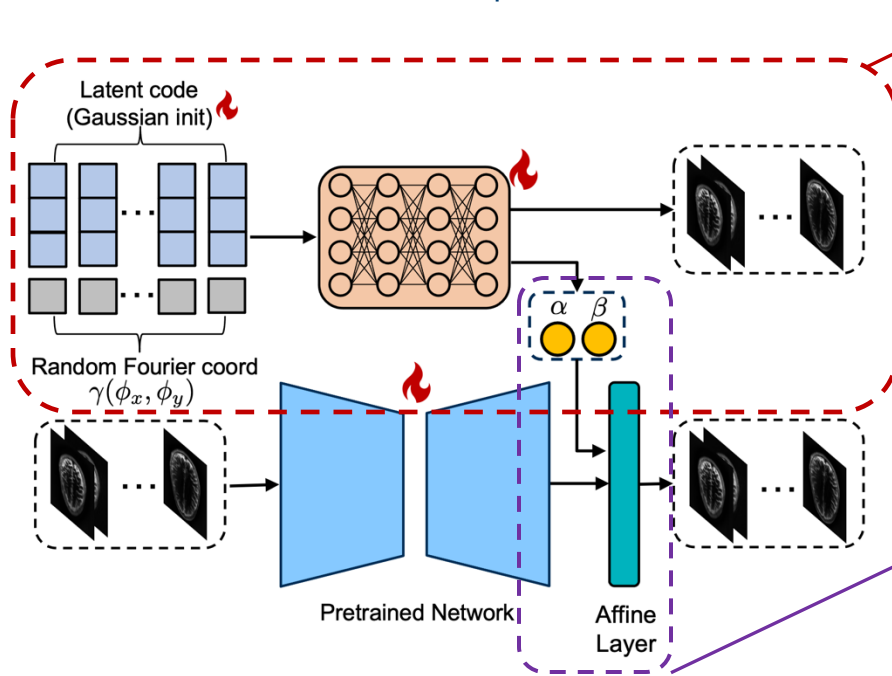
a. Functional-Level Patient Adaptation
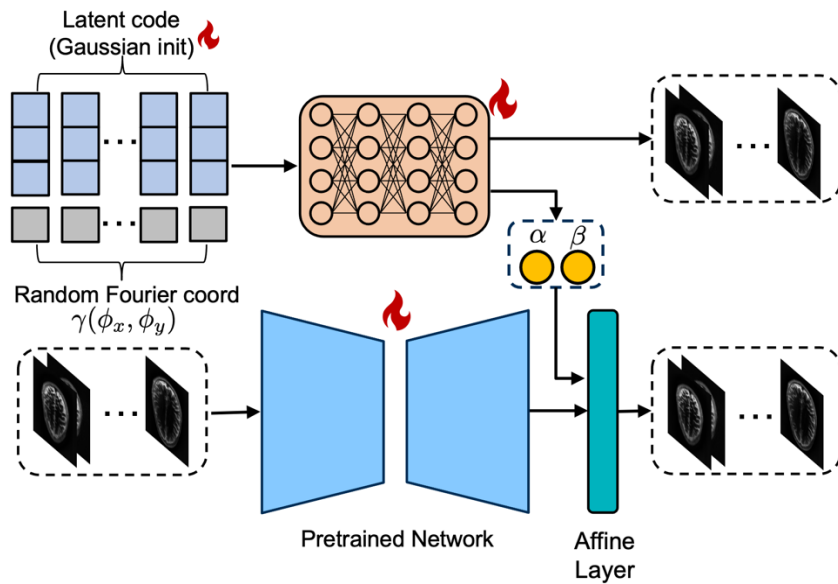
b. Structural-Preserving Single-Slice Refinement (SST)
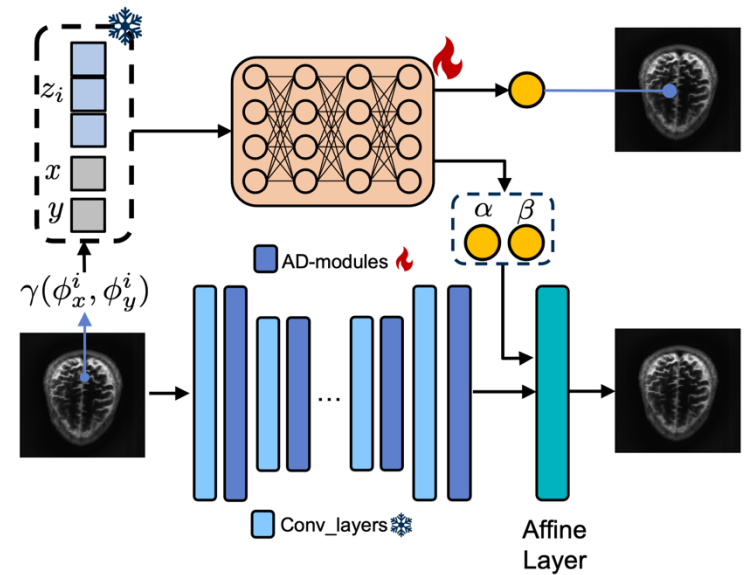
Proposed Method

- D2SA: patient-wise TTA framework
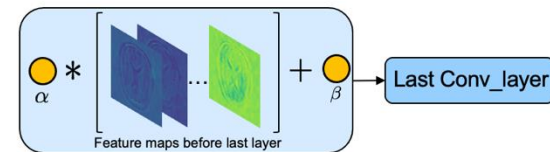
a. Functional-Level Patient Adaptation

➢ MR-INR

$$\tilde{\gamma}(\phi, z_i) = [z_i, \cos(2\pi B\phi), \sin(2\pi B\phi)],$$

Integrate Siren and Fourier feature

$$[\hat{x}, \alpha, \beta] = f_\theta(\tilde{\gamma}(\phi^i, z))$$
$$= W_n(\Gamma_{n-1} \circ \Gamma_{n-2} \circ \cdots \circ \Gamma_0)(\tilde{\gamma}(\phi^i, z)) + b_n,$$
$$h^{(i+1)} = \Gamma_i(h^{(i)}) = \sin(W_i h^{(i)} + b_i),$$

➢ Affine Transformation

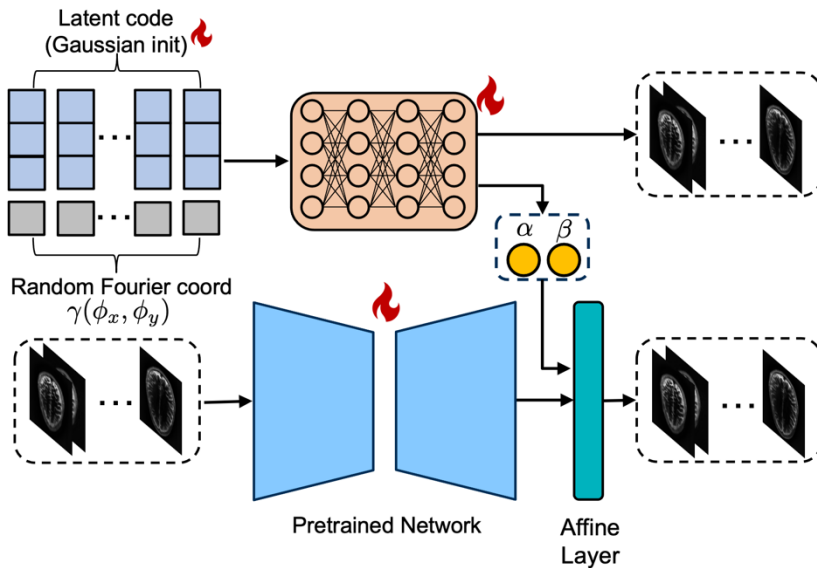1. Learnable variance shifts α
2. Learnable nonzero-mean shifts β

Proposed Method

- D2SA: patient-wise TTA framework

a. Functional-Level Patient Adaptation

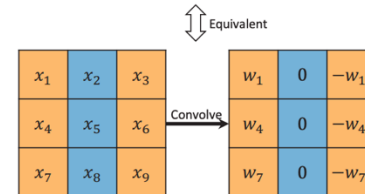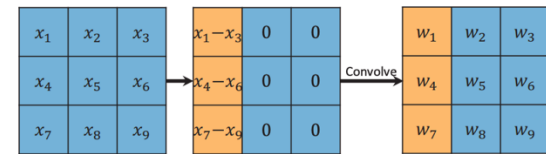Loss Function:

$$\hat{\theta}, \hat{z}, \hat{\Delta} = \arg\min_{\theta, z, \Delta} \lambda_{\text{INR}} \sum_{(x_j, z_j, y_j) \in X} \mathcal{L}_1(Af(\tilde{\gamma}(\phi^j, z), \theta), y_j)$$

$$+ \lambda_{\text{reg}} \frac{1}{\sigma^2} \|z\|_2^2 \quad + \lambda_{\text{self}} \sum_{(x_j) \in X} \mathcal{L}_{\text{self}}(g(x_j, \alpha, \beta, \delta + \Delta)).$$

Proposed Method

- D2SA: patient-wise TTA framework

b. Structural-Preserving Single-Slice Refinement (SST)

Central Difference Convolution (CDC)
Angular Difference Convolution (ADC)
Horizontal Difference Convolution (HDC)
Vertical Difference Convolution (VDC)
Vanilla Convolution (VC)

[1]

[1] Chen Z et al,. "ea-net: Single image dehazing based on detail-enhanced convolution and content-guided attention", IEEE Transactions on Image Processing 2024
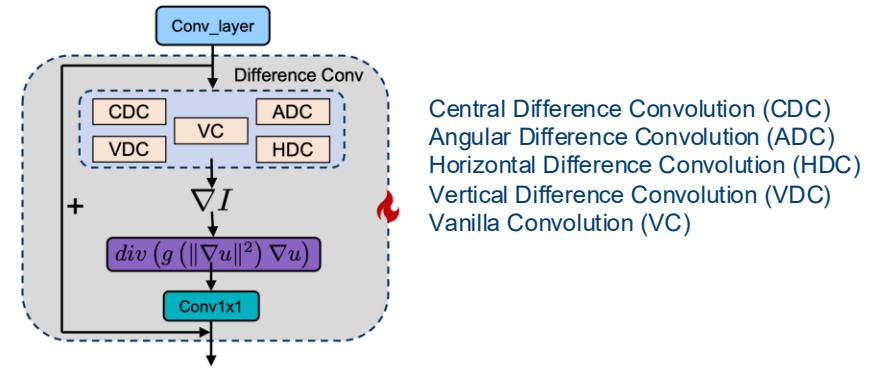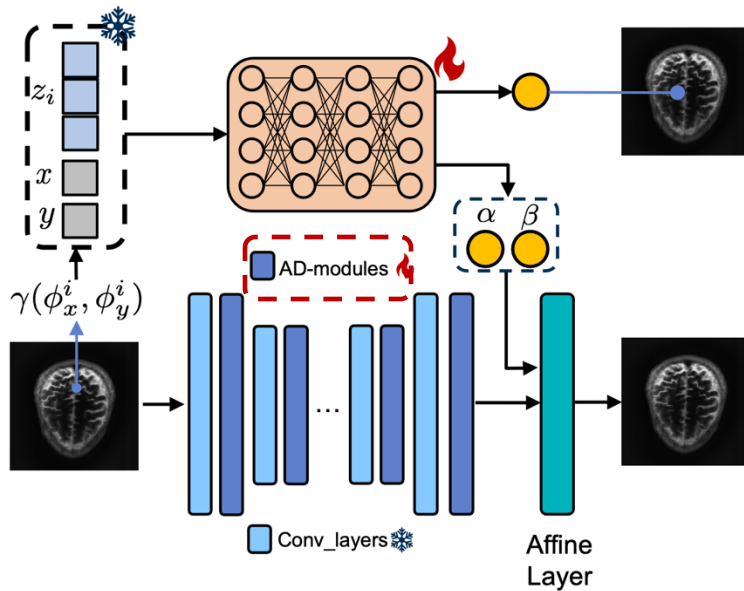
Proposed Method

- D2SA: patient-wise TTA framework

b. Structural-Preserving Single-Slice Refinement (SST)

Central Difference Convolution (CDC)
Angular Difference Convolution (ADC)
Horizontal Difference Convolution (HDC)
Vertical Difference Convolution (VDC)
Vanilla Convolution (VC)

$$\frac{\partial u}{\partial t} = \mathrm{div}\left(g(|\nabla u|)\nabla u\right)$$

$$g(|\nabla u|) = \frac{1}{1 + \frac{|\nabla u|^2}{k^2}}$$

$$\begin{cases} \nabla u = F_{\mathrm{out}} = \mathrm{DConv}(F_{\mathrm{in}}) = \sum_{i=1}^{5} F_{\mathrm{in}} * K_i \\ \\ \quad = F_{\mathrm{in}} * K_{\mathrm{cvt}}, \\ \\ u_{i+1} = u_i + \Delta t \cdot \mathrm{div}\left(g(|\nabla u_i|)\nabla u_i\right) \end{cases}$$

Proposed Method

- D2SA: patient-wise TTA framework
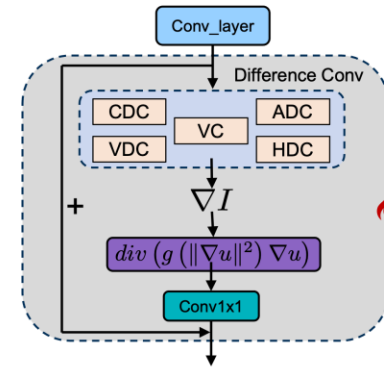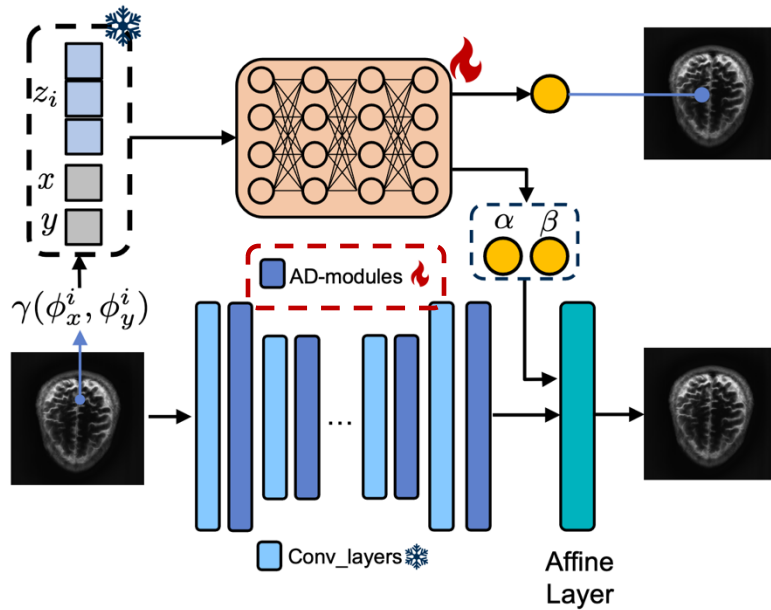
b. Structural-Preserving Single-Slice Refinement (SST)
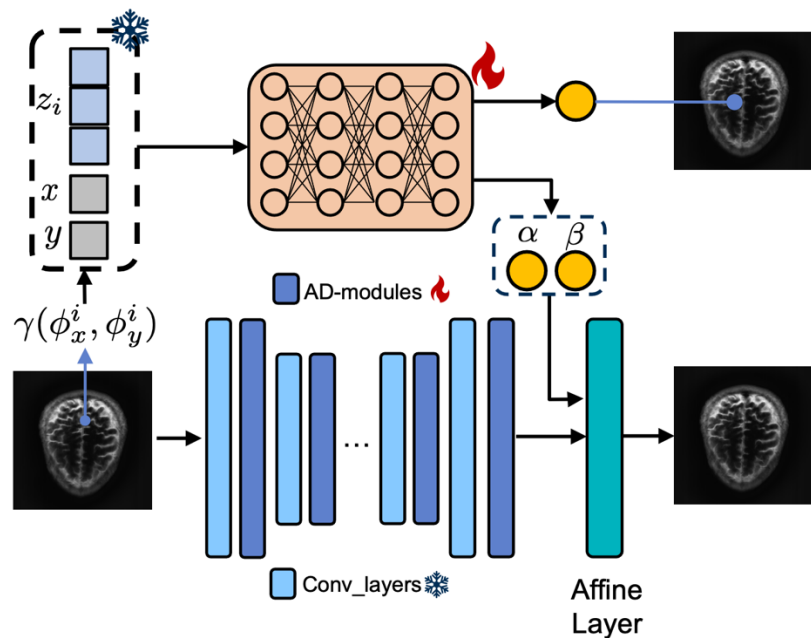
Loss Function:

$$\hat{\theta}, \hat{\Delta} = \arg\min_{\theta, \Delta} \sum_{(x_j, y_j) \in X} \underbrace{\lambda_{\text{INR}} \mathcal{L}_1\big(A f(\tilde{\gamma}(\phi^j, \hat{z}), \theta), y_j\big)}_{\text{MR-INR Recon Loss}}$$

$$+ \sum_{(y_j) \in X} \lambda_{\text{self}} \underbrace{\frac{|y_j - A g(\mathbf{A}^\dagger \mathbf{y}_i, \delta + \Delta)|_1}{|y_j|_1}}_{\text{Self-sup Loss}} .$$

Proposed Method

➢ Mathematical Analysis for Proposed Methods

- We provide a view how the learned parameters α and β enable effective adaptation under distribution shifts. First, consider a target distribution:

$$Q : \mathbf{y} = \mathbf{x} + \mathbf{z}, \ \mathbf{x} = \mathbf{U}\mathbf{c} + \mu_Q, \ \mathbf{c} \sim \mathcal{N}(0, I), \ \mathbf{z} \sim \mathcal{N}(0, s^2 I).$$

- Here, $U \in R^{n \times d}$ is an orthonormal basis for the signal subspace, and μ^Q represents the mean shift in the test distribution with small size. Our goal is to estimate x under this shift. The optimal test-time adaptation estimator is:

$$\hat{\mathbf{x}} = \alpha \mathbf{U}\mathbf{U}^T \mathbf{y} + \beta,$$

- Where α adjusts for variance shifts, and β corrects mean shifts. The self-supervised loss is formulated as:

$$L_{SS}(\alpha, \beta, \mathbf{U}, \mathbf{y}) = \mathbb{E}_Q \left[\|\mathbf{y} - \alpha \mathbf{U}\mathbf{U}^T \mathbf{y} - \beta\|_2^2 \right] + \frac{2\alpha d}{n - d} \mathbb{E}_Q \left[\|(\mathbf{I} - \mathbf{U}\mathbf{U}^T)\mathbf{y}\|_2^2 \right]$$

- Solving for the optimal α^* and β^* by first-order derivatives

$$\alpha^* = \frac{1}{1 + s^2}. \qquad\qquad \beta^* = \mu_Q.$$

- Thus, α and β optimise independently, where α^* dynamically adapts to noise variance shifts, and β^* corrects mean shifts.

Experiment

- Domain shifts (S: Source; T: Target)

  - Anatomy shift (S: Knee and T: brain); FastMRI [1]

  - Dataset shift (S: Stanford-knee and T: FastMRI)

  - Acquisition shift (S: T2, and T: T1pre), FastMRI

  - Acceleration shift (S: 2x and T: 4x); FastMRI

- Compared Methods

  - Single-slice training (SST)

    - DIP-TTT [3]: A single-slice test-time training method based on Deep Image Prior (DIP).

  - Batch-level training (patient-wise training)

    - FINE [4]: A batch TTA technique using fidelity-based constraints

    - Noiser2noise (NR2N) [5, 6] and SSDU [35]: Self-supervised approaches suitable for patient-wise TTA

  - Batch-level training + SST

- Our Methods (pluggable)

  - Stage 1: Functional-Level Patient Adaptation

    - FINE + MR-INR/ NR2N + MR-INR/SSDU+MR-INR

  - Stage 2: Single-Slice Refinement (SST)

    - FINE + MR-INR+SST/ NR2N + MR-INR+SST/SSDU+MR-INR+SST

[1] https://fastmri.med.nyu.edu/
[2] http://mridata.org/list?project=Stanford%20Fullysampled%203D%20FSE%20Knees
[3] D. Mohammad et al., "Test-Time Training Can Close the Natural Distribution Shift Performance Gap in Deep Learning Based Compressed Sensing", ICML, 2022
[4] Zhang J et al., "Fidelity imposed network edit (fine) for solving ill-posed image reconstruction", Neuroimage 2020
[5] Moran N et al., "Learning to Denoise From Unpaired Noisy Data", CVPR 2020
[6] Yaman B et al., "Self-supervised learning of physics-guided reconstruction neural networks without fully sampled reference data", Magnetic resonance in medicine 2020

Experiment

- Main Results

Method (UNet)	Anatomy Shift ($\mathcal{S}$: Knee, $\mathcal{T}$: Brain)	Dataset Shift ($\mathcal{S}$: Stanford, $\mathcal{T}$: fastMRI)	Modality Shift ($\mathcal{S}$: AXT2, $\mathcal{T}$: AXT1PRE)	Acceleration Shift ($\mathcal{S}$: 2x, $\mathcal{T}$: 4x)
Zero-filling	0.737/24.50/0.327/-	0.754/24.33/0.359/-	0.747/25.7/0.350/-	0.754/23.371/0.396/-
Non-TTA	0.625/21.77/0.458/-	0.559/21.87/0.454/-	0.794/27.18/0.391/-	0.726/23.37/0.396/-
DIP-TTT	0.859/27.05/0.322/42.1	0.810/28.08/0.298/40.8	0.846/27.61/0.361/31.5	0.815/27.93/0.299/95.3
FINE	0.834/25.98/0.351/4.9	0.796/26.54/0.319/6.4	0.825/26.71/0.377/5.6	0.782/25.75/0.333/6.6
FINE+MR-INR	0.845/26.37/0.346/5.5	0.807/26.84/0.314/6.6	0.835/26.51/0.373/6.0	0.793/26.29/0.326/7.0
FINE+SST	0.868/27.22/0.327/17.2	0.827/28.16/0.283/21.9	0.853/27.72/0.283/21.9	0.822/28.07/0.689/52.2
FINE+MR-INR+SST	0.876/27.71/0.320/12.1	0.829/28.34/0.279/18.7	0.861/27.93/0.279/15.7	0.825/28.54/0.286/31.9
NR2N	0.836/25.80/0.353/5.2	0.796/26.71/0.316/6.9	0.826/26.59/0.383/6.7	0.781/26.20/0.335/6.9
NR2N+MR-INR	0.849/26.11/0.346/5.7	0.798/26.42/0.317/7.4	0.829/26.64/0.380/7.3	0.791/26.37/0.332/7.5
NR2N+SST	0.868/27.38/0.323/21.7	0.825/28.23/0.284/22.5	0.854/27.69/0.284/22.6	0.822/28.07/0.291/52.7
NR2N+MR-INR+SST	0.871/27.32/0.323/12.2	0.830/28.43/0.279/16.4	0.862/27.98/0.279/14.5	0.825/28.86/0.287/31.7
SSDU	0.851/24.82/0.353/5.4	0.788/22.37/0.344/7.8	0.819/24.27/0.339/7.1	0.789/23.03/0.346/7.3
SSDU+MR-INR	0.861/25.18/0.348/5.6	0.789/22.45/0.339/8.0	0.832/24.97/0.385/7.4	0.797/23.78/0.344/7.7
SSDU+SST	0.871/25.17/0.349/25.3	0.825/28.35/0.284/30.6	0.854/27.71/0.287/25.7	0.823/28.07/0.293/139.8
SSDU+MR-INR+SST	0.877/27.46/0.322/11.5	0.828/28.36/0.287/18.9	0.860/28.04/0.287/17.4	0.826/28.62/0.286/44.2

Table 1. Performance comparison of UNet methods under different domain shifts. Each cell presents (**SSIM** ↑ / **PSNR** ↑ / **LPIPS** ↓ / **Time (mins/patient)** ↓). The family of proposed methods incorporates a self-supervised learning framework, combining MR-INR-based patient-wise adaptation with single-slice refinement using pre-trained patient-wise models.

UNIVERSITY OF CAMBRIDGE

Experiment

- Main Results

Method (VarNet)	Anatomy Shift ($\mathcal{S}$: Knee, $\mathcal{T}$: Brain)	Dataset Shift ($\mathcal{S}$: Stanford, $\mathcal{T}$: fastMRI)	Modality Shift ($\mathcal{S}$: AXT2, $\mathcal{T}$: AXT1PRE)	Acceleration Shift ($\mathcal{S}$: 2x, $\mathcal{T}$: 4x)
Zero-filling	0.737/24.50/0.327/-	0.747/24.33/0.359/-	0.747/25.71/0.350/-	0.754/23.37/0.396/-
Non-TTA	0.799/23.16/0.371/-	0.706/22.35/0.365/-	0.796/23.54/0.379/-	0.761/23.04/0.372/-
DIP-TTT	0.878/27.67/0.312/52.5	0.798/28.02/0.292/41.8	0.867/28.33/0.337/71.6	0.815/28.25/0.285/137.2
FINE	0.820/24.01/0.343/3.9	0.789/26.26/0.311/6.6	0.821/26.18/0.369/3.5	0.696/21.39/0.342/6.2
FINE+MR-INR	0.862/26.45/0.328/4.7	0.795/26.44/0.306/6.9	0.830/26.58/0.369/4.4	0.791/25.30/0.310/7.5
FINE+SST	0.862/27.57/0.311/53.5	0.794/27.72/0.294/20.3	0.857/28.08/0.345/79.8	0.823/28.17/0.288/63.8
FINE+MR-INR+SST	0.882/27.68/0.311/17.1	0.808/28.72/0.286/18.2	0.867/28.32/0.337/21.8	0.829/28.64/0.276/44.5
NR2N	0.827/23.95/0.334/4.9	0.798/26.59/0.299/6.8	0.827/25.60/0.368/4.1	0.718/20.97/0.327/6.6
NR2N+MR-INR	0.868/26.41/0.321/5.1	0.806/26.95/0.294/7.1	0.833/26.44/0.369/4.7	0.806/25.42/0.291/7.6
NR2N+SST	0.883/27.72/0.307/63.9	0.798/27.78/0.293/25.3	0.860/28.17/0.341/80.2	0.822/28.09/0.291/69.2
NR2N+MR-INR+SST	0.884/27.81/0.306/18.7	0.812/28.76/0.281/20.4	0.869/28.36/0.336/20.3	0.826/28.89/0.273/43.1
SSDU	0.738/20.87/0.375/5.1	0.737/20.43/0.349/7.2	0.746/22.59/0.391/4.4	0.556/16.93/0.421/7.4
SSDU+MR-INR	0.821/23.25/0.350/5.3	0.764/21.67/0.339/7.5	0.796/24.09/0.390/4.8	0.728/19.57/0.358/7.9
SSDU+SST	0.879/27.65/0.310/68.3	0.789/26.79/0.299/24.9	0.857/28.07/0.343/93.4	0.803/28.06/0.293/134.2
SSDU+MR-INR+SST	0.882/27.66/0.307/18.5	0.808/28.16/0.290/21.4	0.863/28.09/0.342/29.3	0.826/28.62/0.286/45.2

Table 2. Performance comparison of VarNet methods under different domain shifts. Each cell presents ((**SSIM** ↑ / **PSNR** ↑ / **LPIPS** ↓ / **Time (mins/patient)** ↓). The family of proposed methods incorporates a self-supervised learning framework, combining MR-INR-based patient-wise adaptation with single-slice refinement using pre-trained patient-wise models.

UNIVERSITY OF CAMBRIDGE
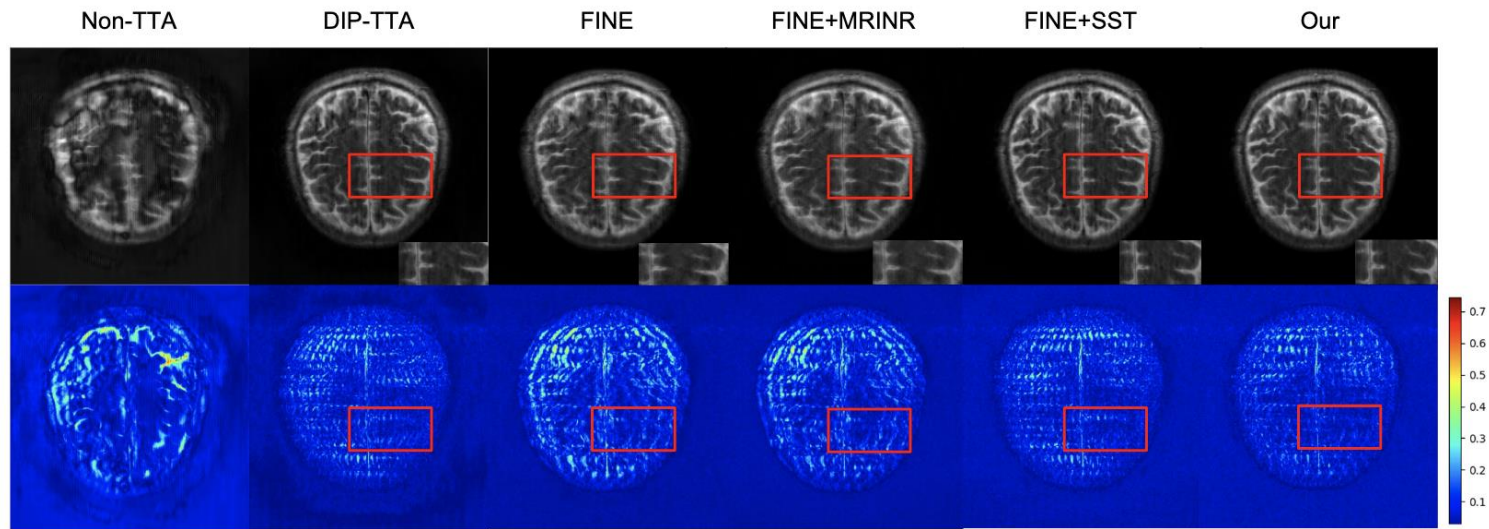
Experiment

- Qualitative Results-UNet

Figure 4. Comparison of different frameworks in UNet under anatomy shift (Knee to Brain) using the FINE method. The first row shows reconstructed MRI images, while the second row presents residual maps between reconstructions and full-sampled MRI. The proposed method (far right) achieves the lowest residuals, indicating improved reconstruction accuracy
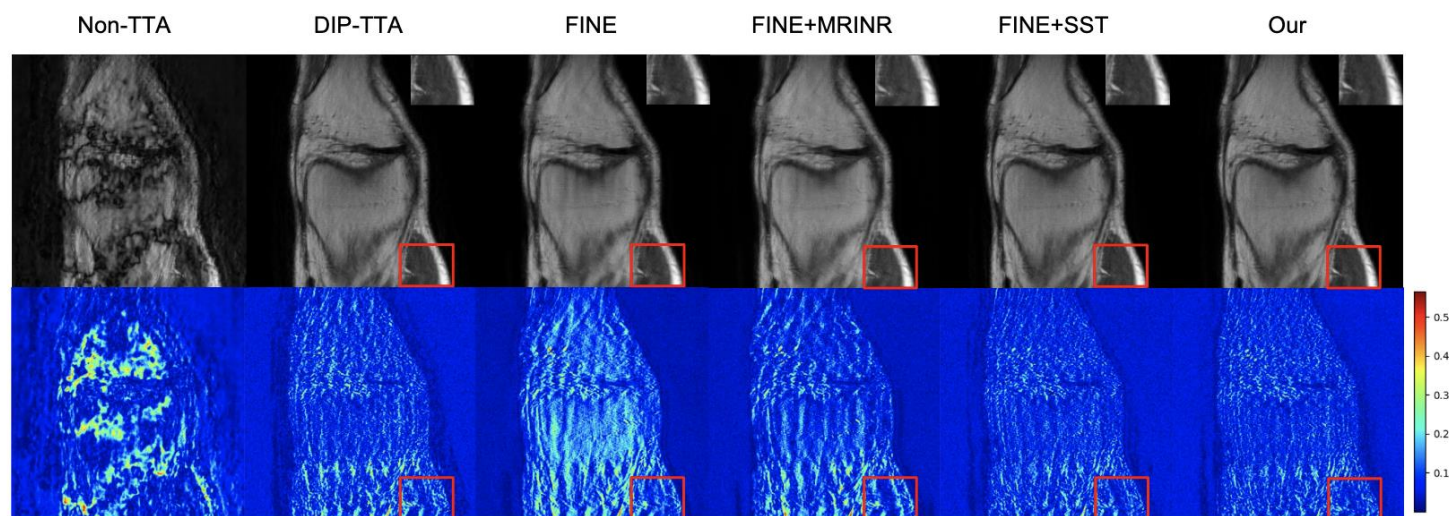
Experiment

- Qualitative Results-VarNet

Figure 5. Comparison of different frameworks in VarNet under dataset shift (Stanford to fastMRI) using the FINE method. The first row shows reconstructed MRI images, while the second row presents residual maps between reconstructions and full-sampled MRI. The proposed method (far right) achieves the lowest residuals, indicating improved reconstruction accuracy

Experiment

- ## Ablation studies-UNet (anatomy shift)

Stage	Method (UNet)	Knee → Brain
Patient-wise training	FINE	25.98/31.02/4.9
	+MR-INR + fixed latent code	26.37/31.29/5.3
	+MR-INR + learnable latent code	26.48/31.29/5.5
Single-slice training (SST)	+SST (learnable conv layers; no AD module)	27.22/31.02/17.2
	+MR-INR+SST (learnable conv layers; no AD module)	27.65/31.29/23.65
	+MR-INR+SST (learnable conv layers + AD module)	27.54/46.13/15.7
	+MR-INR+SST (Frozen conv layers + AD module)	27.71/17.89/12.1

Table 3. Ablation study on MR-INR and the AD module under anatomy shift (Knee to Brain) using UNet. Metrics are **PSNR/ Number of Parameters (M, Millions) / Time per Patient (min)**. The first stage evaluates MR-INR with fixed and learnable latent codes (1408 parameters). The second stage compares SST configurations with MR-INR and AD.

- ## Different INR-UNet (anatomy shift)

Stage	INR-Network	Knee → Brain
Patient-wise training (FINE+MR-INR)	Random PE+MLP	0.845/25.76/0.349
	WIRE	0.839/25.78/0.354
	Only SIREN	0.845/26.16/0.349
	Our (Random PE+SIREN)	**0.845/26.37/0.346**
Single-slice training (FINE+MR-INR+SST)	Random PE+MLP	0.864/27.22/0.326
	WIRE	0.872/27.44/0.321
	Only SIREN	0.874/27.51/0.322
	Our (Random PE+SIREN)	**0.876/27.71/0.320**

Table 1: Ablation study on INR design under anatomy shift (Knee to Brain) using UNet. Metrics are **SSIM/PSNR/LPIPS**. The first stage evaluates MR-INR with different implicit neural representations. The second stage compares SST configurations with MR-INR using different backbone architectures.
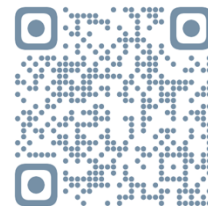
- ## Impact of different learning rates

Table 1: UNet (Dataset Shift; Fine) — PSNR/SSIM/LPIPS

Learning Rate	Functional-Level Patient Adaptation		Structural-Preserving Single-Slice Refinement	
	FINE PSNR/SSIM/LPIPS	**FINE+MR-INR** PSNR/SSIM/LPIPS	**FINE+SST** PSNR/SSIM/LPIPS	**FINE+MR-INR+SST** PSNR/SSIM/LPIPS
1e-3	0.768/24.41/0.352	0.772/24.96/0.345	0.806/27.18/0.304	0.821/27.64/0.276
1e-4	0.796/26.54/0.319	0.807/26.84/0.314	0.827/28.16/0.283	0.829/28.34/0.279
1e-5	0.785/26.18/0.329	0.787/25.78/0.323	0.821/28.01/0.280	0.826/28.05/0.289

UNIVERSITY OF CAMBRIDGE

Conclusion

➤ More results in paper and supplementary

  o Quantitative results of same domain shifts

  o Qualitative results of other methods (NR2N, SSDU)

  o Detail of mathematical analysis …….

➤ **Dual-Stage Distribution and Slice Adaptation (D2SA),** a test-time adaptation framework that enhances MRI reconstruction under distribution shifts.

➤ Leverage **MR-INR**, D2SA performs patient-wise adaptation to model **mean/variance shifts**

➤ Use a **learnable anisotropic diffusion (AD) module** in structure-preserving single-slice refinement.

➤ Extensive Validation on **multiple domain shifts**

UNIVERSITY OF CAMBRIDGE

University of Cambridge

Thank you!